JOURNAL OF MATERIALS SCIENCE 32 (1997) 4523–4531

Structure–property relationships in polyethylene blends: the effect of morphology on electrical breakdown strength

I. L. HOSIER, A. S. VAUGHAN*
J. J. Thomson Physical Laboratory, University of Reading, Whiteknights, Reading RG6 6AF, UK

S. G. SWINGLER
The National Grid Company plc, Technology and Engineering Division, Kelvin Avenue, Leatherhead KT22 7ST, UK

Blends of linear and branched polyethylene were prepared covering the composition range 1–20% linear polyethylene, and three thermal treatments were subsequently chosen to produce a range of different morphologies. Isothermal crystallization at 124 °C gives rise to compact linear inclusions within a matrix of branched polyethylene, isothermal crystallization at 115 °C produces an open, banded spherulitic morphology and, finally, quenching leads to a continuous spherulitic texture. Ramp testing was then employed to investigate the effect of morphology on electrical strength. It was found that the electrical strength of the blend depends primarily on the morphology and that, by optimizing thermal treatment and linear polyethylene content, substantial improvements in properties can be obtained.

1. Introduction

Blending of two or more polymers constitutes an attractive means of controlling macroscopic physical properties and, as a result, this topic has attracted a great deal of interest [1–3]. In the case of blends of linear (LPE) and branched polyethylene (BPE), isothermal crystallization at temperatures above those where extensive crystallization of the branched component takes place, leads to the formation of spherulites containing lamellar crystals that are rich in the linear polymer [4, 5]. Although a degree of co-crystallization inevitably does occur, to a first approximation, the linear component can be thought of as crystallizing from a solution, where the "solvent" is the branched polymer. As a consequence of this, a wide range of morphologies [6, 7] can be produced in these systems, with thermal treatment and composition being the variables used to control the final microstructure.

Dielectric breakdown in polymers is a subject which is of great academic and technological interest. However the factors that contribute to a breakdown event are many and varied and may include space charge injection [8], impurities and additives [9], defect structures [10], material parameters [11] etc. Although it is generally understood that failure occurs when a conducting pathway bridges the dielectric, the mechanisms that lead to this are complex [12, 13]. In the absence of polar solvents, a conducting pathway propagates and lengthens through the action of microdischarges, to form what is termed an electrical tree. Although it is appreciated that structural factors can influence this process [13], few attempts have been made to study this area in detail; most investigations have adopted crude approaches to the topic of polymer morphology (see for example references 14–16). Despite this reservation, a number of papers published in the late 1970s and early 1980s are of particular relevance to the work reported here. In these, a correlation between spherulitic development and dielectric strength was reported [16–18] and it was argued that the regions between spherulites dominate the breakdown behaviour. Hence, spherulitic development leads to reduced electrical strength. Although a number of possible explanations were proposed to account for this behaviour [18], the true reason remained unclear.

The work described here set out to re-examine such issues in the light of current understanding of crystallization and morphology in polyethylene. By making use of the control of structural parameters that is achievable in polymer blends, it is possible to study systematically and independently, the influences

* Author to whom correspondence should be addressed.

0022–2461

morphology and molecular composition have on dielectric breakdown. In this paper, attention will be focused on the role of morphology.

2. Experimental procedure

2.1. Materials

All of the blends described below were prepared from the linear polyethylene Rigidex 140/60 (BP Chemicals, $M_w = 53\,000$ $M_n = 16\,000$) and the super-clean low density branched polyethylene 4901 (Borealis Polymers, $M_w = 76\,800$ $M_n = 11\,300$), using the following solvent blending procedure. The two polymers were first weighed in the required proportions and added to xylene to give a 1% w/v solution. This was then heated to around 140 °C, with vigorous stirring. When all the polymer had dissolved, the solution was poured into an excess of cold methanol, whereupon the polyethylene precipitated out. After filtration and vacuum drying, the homogeneity of the blend was investigated using optical microscopy and differential scanning calorimetry (DSC). No inhomogeneities were found using either of these techniques.

2.2. Sample preparation

Samples for detailed morphological study were prepared by melt pressing, followed by either isothermal crystallization in a Mettler FP5 hot stage, or quenching directly from the melt into ice/water. For all the isothermal samples, the crystallization time was chosen such that the linear component crystallized to the maximum extent (see below), and for convenience, all samples will subsequently be referred to using the following general notation; BPA T/C. In this, BPA signifies blended polyethylene type A (i.e. one composed of 140/60 and 4901), T defines the thermal treatment used, and C the percentage of linear polyethylene. Thus, for example, BPA 124/20 contains 20% 140/60 and was crystallized at 124 °C, whereas BPA Q/1 only contains 1% of the linear material and was quenched directly from the melt.

Samples for electrical testing were chosen to be of the order of 70 μm in thickness to ensure that the required voltage for breakdown was well within the limitations of the electrical testing equipment. Previous studies suggested that, for reproducible results to be obtained, it is essential that all samples are of a constant and uniform thickness, since sample thickness is known to affect the measured electrical strength [19, 20]. Therefore, to obtain the necessary sample uniformity, a slightly different processing route was employed from that described above. A Grasby-Specac 25.011 hydraulic press equipped with a thin film maker was used to give the sample thickness and uniformity required, and to provide a means of initially melting the specimens. These thin film specimens were subsequently crystallized between adherent aluminium foils in a Grant W28 temperature controlled silicone oil bath. Despite this modified production route, comparison of the electrical test specimens with those intended for detailed morphological study revealed no significant structural differences.

2.3. Characterization

A differential scanning calorimeter, Perkin Elmer model DSC-2C, was used both to identify the time required in each system for maximum crystallization of the linear component, and to probe the lamellar structure of each blend after isothermal crystallization. To identify the required crystallization time, samples of the untreated blend were melted in the DSC and data were collected continuously (during cooling from the melt and during isothermal crystallization) until crystallization was complete. Subsequent melting endotherms were collected at a scan rate of 10 K min^{-1}; typically 3–4 mg samples were employed throughout.

Selected samples were prepared for electron microscopy, using the following procedure. After microtomy, the exposed surface was etched using a permanganic reagent composed of 1% (w/v) of potassium permanganate dissolved in an acid mix containing 10 parts sulphuric acid to 4 parts orthophosphoric acid to 1 part water; the specimens were recovered following established procedures [21]. After etching, some samples were gold coated for optical or scanning electron microscopy (SEM, Phillips 515). Alternatively, a standard two-stage technique was used to prepare shadowed carbon replicas [22] for more detailed morphological studies in the transmission electron microscope (TEM, Phillips 301).

2.4. Electrical test procedure

Samples prepared for electrical testing were first vacuum dried to remove any water, which may influence the measured electrical strength [23]. Twenty tests were then performed on each batch of samples and, from these data, the electrical strength (mean plus 95% confidence intervals) was calculated assuming a normal distribution. Re-examining the results using Weibull analysis [24] did not affect the observed variations. A standard electrical test procedure was used [13], based upon the general considerations laid down in the ASTM standard D 149–87. A thin film sample was immersed in Dow Corning silicone oil (200/20cs) between opposing 6.3 mm diameter steel ball-bearing electrodes and a 50 g load applied to the upper electrode. The lower electrode was connected to earth, and an increasing voltage (a.c. 50 Hz) applied to the upper ball-bearing electrode until the sample failed. All the data presented here were acquired at a ramp rate of 50 V s^{-1}, as the effect of ramp rate on breakdown strength is not clear [24]. All experimental parameters were computer controlled and appropriate data were logged automatically.

3. Results and discussion

3.1. Preliminary studies

Before embarking on any detailed investigation, a number of preliminary studies were performed. Although dissolution in xylene has been used extensively as means of preparing polyethylene blends [4–7], the likely effects of our chosen procedure on both the

structure and, more critically, the electrical properties of the resulting materials were first investigated. This was accomplished by comparing the virgin BPE with the same polymer after dissolution in xylene and recovery, as described above. No significant structural differences were revealed by DSC or microscopy. Also, the electrical strength of the BPE was unaffected by the dissolution process (virgin BPE, breakdown strength $130 \pm 5\,kV\,mm^{-1}$; xylene processed BPE, $128 \pm 4\,kV\,mm^{-1}$). The same conclusion has been reported in other studies [25, 26].

Samples crystallized within the temperature range 110–127 °C were then examined optically, both in the Mettler hot stage during crystallization (in this way crystallization times could be estimated) and following permanganic etching. Two morphological regimes were found. At temperatures above about 118 °C, morphologies are based upon compact, sheaf-like, lamellar aggregates whereas, below this temperature, increasingly open banded spherulites develop. In all samples, these structural entities were uniformly distributed throughout the specimen. On the basis of the results described above, isothermal crystallization at 115 and 124 °C were chosen to be representative of open spherulitic and compact sheaf-like inclusions respectively. In quenched systems, little structural detail could be seen optically and the observed uniform texture did not appear to change appreciably with composition.

3.2. Differential scanning calorimetry

3.2.1. Crystallization behaviour

Before any samples could be prepared for detailed investigation, it was necessary to quantify the required crystallization times. Fig. 1a shows how the time for maximum crystallization of the LPE varies as a function of the blend composition and temperature. Thus, higher temperatures as well as lower linear contents require longer crystallization times, in line with expectations [4, 27]. Assuming that the time for maximum crystallization at each temperature is inversely related to the crystallization rate, the measured crystallization times are not inconsistent with secondary nucleation theory [28] (see Fig. 1b). Although the minimum time for "complete" linear crystallization varies with composition, for simplicity, it was decided to adopt crystallization times of 45 min at 115 °C and 4 h at 124 °C. This is sufficient to ensure maximum LPE crystallization in all cases. This procedure also has the advantage of allowing any stress or compositional variations associated with crystallization to relax prior to quenching [29–31].

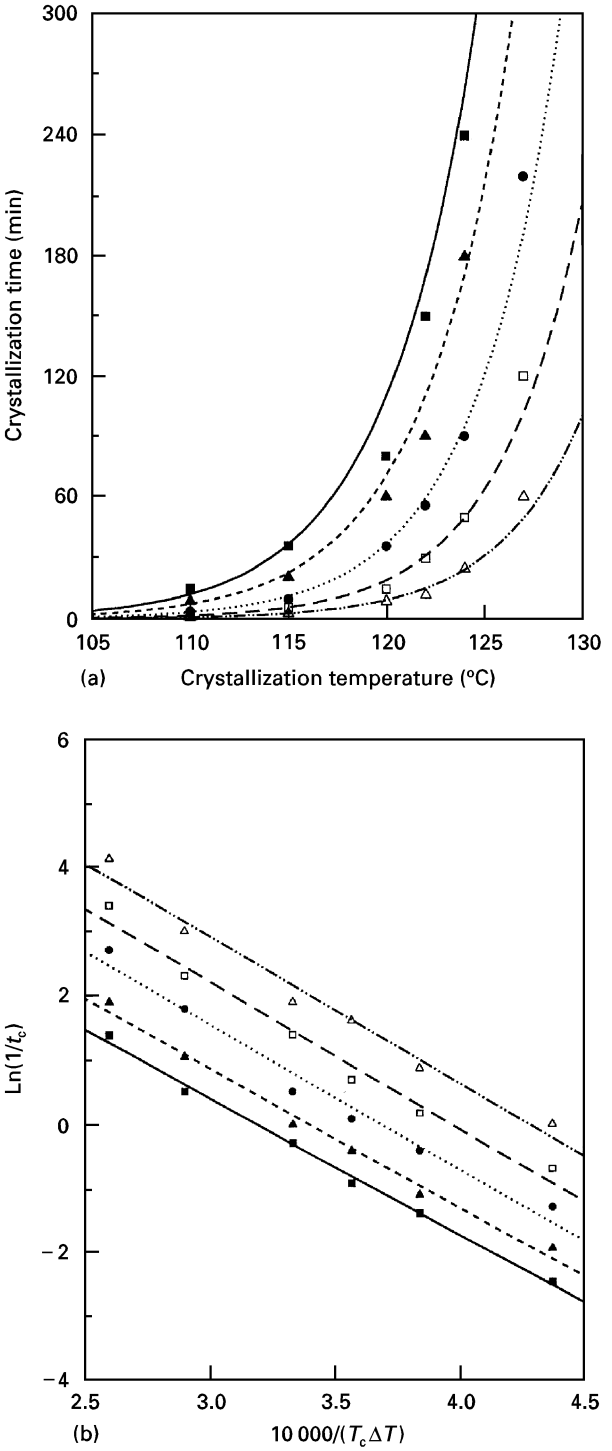

Figure 1 Variation in the time required for complete crystallization (t_c) of the LPE as a function of crystallization temperature (T_c) and blend composition: (■) 1% LPE; (▲) 3% LPE; (●) 7% LPE; (□) 10% LPE; (△) 20% LPE. (a) Plot of raw data; (b) analysis of above in line with secondary nucleation theory ($\triangle T$ is the supercooling below the equilibrium melting temperature T_m°).

3.2.2. Melting behaviour

Fig. 2 shows the melting behvaiour of the quenched samples as a function of LPE content. Two peaks are seen in all the blends, the upper peak being relatively sharp, whereas the lower exhibits a long tail extending towards room temperature. In all the blends, the lower peak maximum is situated at a temperature close to that of the pure BPE, and this feature is therefore associated with lamellae composed *principally* of branched molecules. Subsequently, we shall refer to this lamellar population as the BPE-rich phase. Similarly, the higher melting peak is *principally* associated with linear material (LPE-rich phase).

In the samples crystallized at 115 °C (Fig. 3), the higher temperature peak is generally much narrower and the peak area much higher than in the comparable features in Fig. 2. Indeed, in each case, the enthalpy

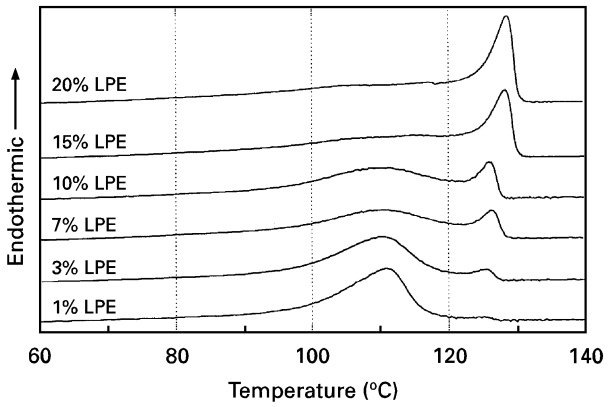

Figure 2 DSC melting behaviour of samples quenched directly from the melt, as a function of blend composition.

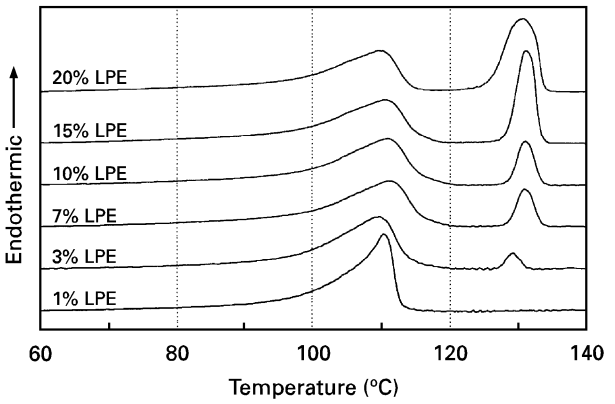

Figure 4 DSC melting behaviour of samples isothermally crystallized at 124 °C, as a function of blend composition.

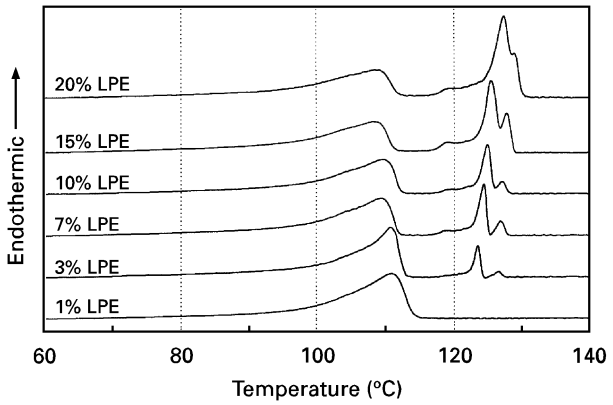

Figure 3 DSC melting behaviour of samples isothermally crystallized at 115 °C, as a function of blend composition.

of this peak is such that it provides strong evidence of co-crystallization of the linear material and the more linear fractions of the BPE, since the observed peak areas would require in excess of 95% of the available LPE to have crystallized prior to quenching. The corresponding peak maximum temperature increases somewhat with linear content (from 123 to 127 °C) and, in addition, at least one subsidiary peak becomes evident. The magnitude of the highest temperature peak is found to be dependent upon the DSC scan rate and this feature can therefore be attributed to a population of lamellae that are richer in LPE and which can therefore reorganize during scanning. The BPE-rich phase seems to be very similar to that which is formed on quenching directly from the melt.

Fig. 4 shows the DSC data obtained from the blends crystallized at 124 °C. The composition and melting point of the BPE-rich lamellae are similar to that discussed above; however, the peak corresponding to the LPE-rich phase is now wider and is singular, in contrast to the samples crystallized at 115 °C. The area of this peak is lower than that of the corresponding endotherm seen in the 115 °C samples, and the melting temperature is around 130 °C, i.e. the two peaks are more widely separated. Thus, crystallization at 124 °C gives two very different lamellar populations, as would be anticipated, and also leads to less co-crystallization.

The results described above lead directly to the following conclusions: (i) since the DSC traces shown in Figs. 2–4 are similar to those reported in the literature (see for example reference 32), it is clear that the materials considered in this study are not atypical; (ii) there is no evidence to suggest that the BPE-rich phase in the BPA 124/C and BPA 115/C sample sets varies to any appreciable degree with thermal treatment or blend composition, only the LPE-rich phase becomes modified as a consequence of changes in crystallization conditions or blend composition. In all materials, the BPE-rich phase appears very similar to the pure 4901.

This second point is particularly important in the context of this investigation since it strongly suggests that a range of morphological features, differing in size and internal texture, can indeed be grown within a largely invariant matrix. Thus, for the first time, the *direct* influence of structural elements, such as spherulites on dielectric breakdown, can be deconvoluted from concomitant but *indirect* molecular effects associated with, for example, rejection of impurities to inter-spherulitic regions.

3.3. Morphological examination

In line with the above DSC results, the morphologies observed throughout this study were similar to those reported elsewhere in the literature. Only a few typical examples are therefore included here and these have been chosen specifically to illustrate key morphological features that have a bearing on the breakdown behaviour described in the following section. Fig. 5 shows two SEM micrographs of samples crystallized at 115 °C. BPA 115/3 (Fig. 5a) contains open banded spherulitic structures (LPE-rich phase) which are about 20 μm in diameter and which are separated from each other by regions of quenched matrix (BPE-rich phase). If the linear content is increased, as in Fig. 5b (BPA 115/15), then the spherulites become more compact, somewhat larger and impinge upon one another such that the banded texture becomes space filling.

Fig. 6 shows the morphology of BPA 115/20, as imaged by TEM. In this micrograph well developed

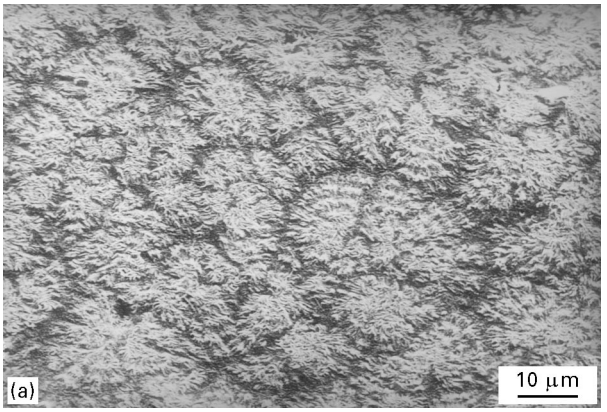

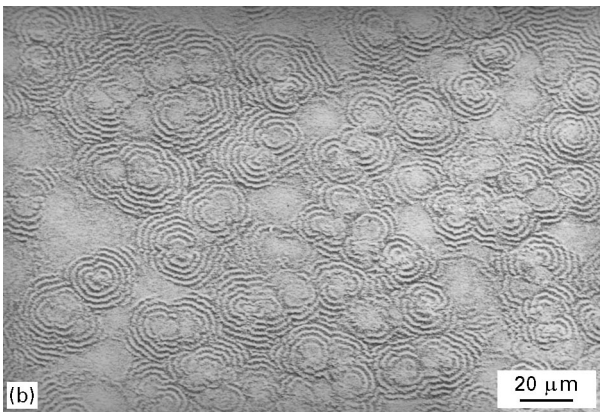

Figure 5 SEM micrographs showing the effect of LPE content on the morphology of blends crystallized at 115 °C: (a) 3% LPE; (b) 15% LPE.

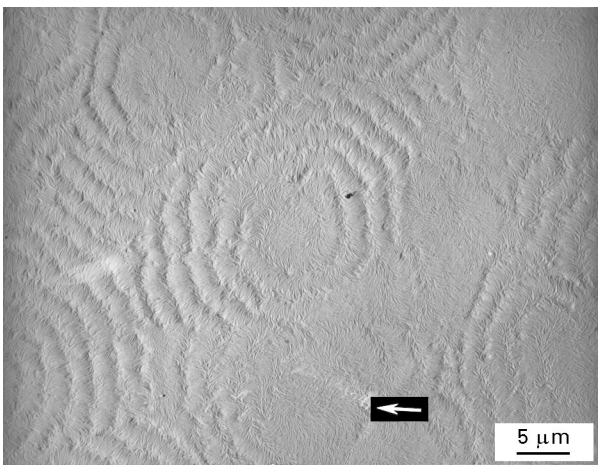

Figure 6 TEM micrograph showing the space-filling, banded spherulitic morphology of sample BPA 115/20 (20% LPE).

banded spherulitic structures are again evident, together with a less obviously banded region (arrowed). However, since no variation of lamellar sizes is apparent here and the lamellae do show orientational correlations, this arrowed region is likely to correspond to another spherulite viewed radially. Thus Fig. 6 confirms that, at 20% LPE content, the morphology is composed of a space-filling, interpenetrating set of spherulites, without any distinct BPE rich matrix. In this case, the BPE is located primarily between the LPE-rich lamellae.

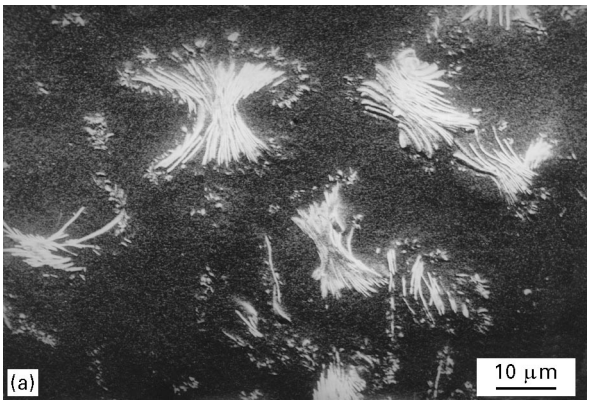

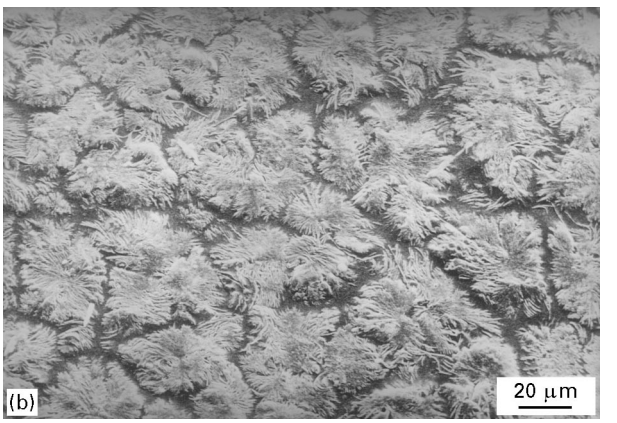

Figure 7 SEM micrographs showing the effect of LPE content on the morphology of blends crystallized at 124 °C: (a) 3% LPE; (b) 15% LPE.

At 124 °C, morphologies are based upon more compact LPE-rich inclusions which, at low linear contents, (3%) are isolated (Fig. 7a). Again, on increasing the percentage of LPE, these inclusions become larger and more numerous, such that in BPA 124/15 they almost impinge (Fig. 7b). However, even at this composition, distinct boundary regions are still evident (compare Figs 5b and 7b). Fig. 8 shows two TEM micrographs of BPA 124/20. From Fig. 8a it is clear that this material contains compact sheaf-like spherulites that are composed of a dense array of radiating LPE-rich lamellae. Significantly, even at 20% LPE, distinct boundary regions still exist (cf. Fig. 6). Fig. 8b shows, at a higher magnification, the distinction between the sizes of the lamellae within a spherulite and those located in the interspherulitic BPE-rich matrix.

SEM examination of quenched blends was not revealing and, therefore, only TEM data are included here. Fig. 9 (BPA Q/20) shows the banded spherulitic morphology that is typical of the quenched specimens. This did not appear to vary appreciably with blend composition.

Based on all the morphological results described above, the following conclusions can now be drawn.

(i) The morphologies shown in Figs 5–9 are broadly in line with those previously reported in the literature. This supports our previous conclusion that the materials under investigation here are not atypical.

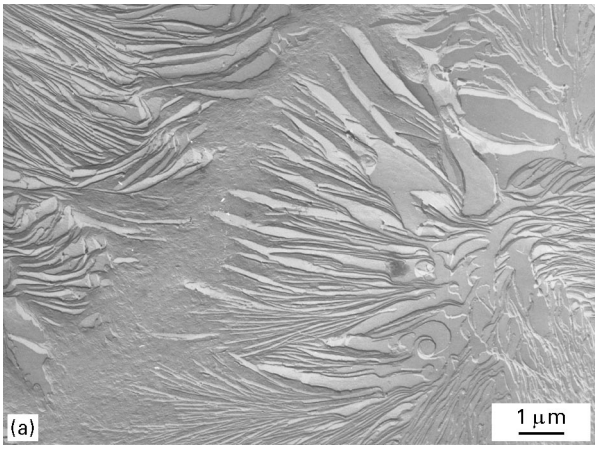

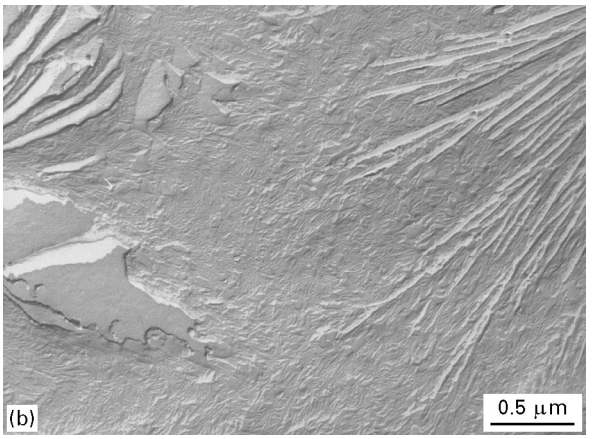

Figure 8 TEM micrographs showing the morphology of sample BPA 124/20 (20% LPE). From (a) it is clear that distinct boundary regions exist between the lamellar aggregates that grow at 124 °C; (b) these inter-spherulitic regions contain small lamellae.

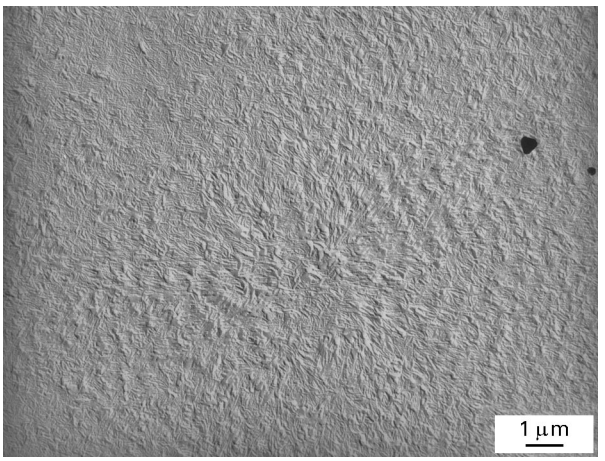

Figure 9 TEM micrograph showing a banded spherulitic morphology, which is typical of all the quenched specimens.

(ii) We observe that, in both of the isothermally crystallized sample sets, the number and size of the linear rich structures increase with linear content and this higher nucleation density, together with the increased availability of crystallizable molecules, could explain why the crystallization time is reduced for blends containing a higher proportion of linear polymer. In the quenched samples, the number and size of banded spherulites do not show any definite trends, since the morphology does not vary appreciably over the blend composition range considered here. Clearly, as required, a range of morphological features can be produced by appropriately choosing the blend composition and crystallization temperature.

(iii) However, the fact that well defined spherulites were observed within the pure BPE and also the quenched blends, but not in the BPE-rich phase in the isothermally crystallized specimens is significant. Despite the DSC evidence, isothermal crystallization of the LPE must modify the surrounding, non-crystallizable branched material to some extent; the inter-spherulitic matrix is *not* identical to the quenched BPE.

3.4. Electrical test results

Fig. 10 shows the average breakdown strength of the blend systems described above. The branched polymer 4901 was found to have a mean electrical strength of $129\ \mathrm{kV\,mm^{-1}}$ and in the analysis that follows, we shall take this as a reference point with which to compare each of the blends. In all cases, appreciable scatter was observed in the results and therefore 95% confidence limits were calculated from each data set; these were found to be of the order of $\pm 5\ \mathrm{kV\,mm^{-1}}$ in every material. Despite this, it is, nevertheless, still possible to identify general trends in the results. In the

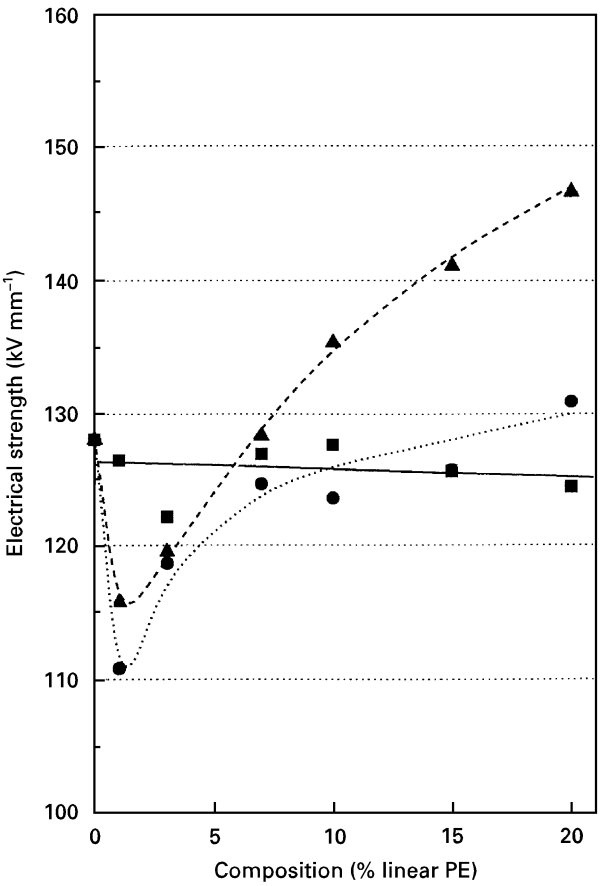

Figure 10 Variation in electrical strength as a function of blend composition and thermal history: (■) quenched samples; (▲) samples crystallized isothermally at 115 °C; (●) samples crystallized at 124 °C.

case of the samples crystallized at 115 °C (open banded spherulites), the electrical strength initially drops, then increases markedly with the proportion of LPE in the blend; a somewhat smaller increase is also seen in the samples crystallized at 124 °C (compact sheaf-like structures). Conversely, in the quenched materials, the electrical strength is largely independent of composition. Compared with the BPE alone, a clear improvement in properties is seen above about 7% LPE in the samples prepared at 115 °C, whereas, in those prepared at 124 °C, a slight improvement could be said to occur above about 17% LPE. Below these limits, both data sets reveal a reduction in electrical strength. Thus, morphologies based upon small well-distributed LPE-rich inclusions lead to lower breakdown strength, whereas space-filling spherulitic structures can improve substantially the electrical strength of the material.

To explain these results it is necessary, first, to consider current understanding of the factors that may influence the breakdown behaviour of a semicrystalline polymer. During a breakdown event, the energy dissipated locally is substantial and, for this reason, it has been argued that the lamellar texture can only ever play a minor role in influencing electrical strength [24, 33]. Conversely, detailed TEM studies of electrical tree *initiation* have suggested that, in the earliest stage of development, the tree does not grow in the direction of the maximum electric field but, rather, tends to develop parallel to the neighbouring lamellae [34, 35]; that is, the lamellae appear to serve as barriers which deflect the growing tree. Clearly this phase of the breakdown process seems to be affected by the spatial distribution of lamellae in the vicinity of the initiation site. In view of this, it is easy to see how a space-filling spherulitic texture could result in improved properties. In polyethylene blends, spherulites are composed of an array of linear-rich lamellae separated by regions of branched material. Electrically, such a morphology effectively constitutes an interpenetrating array of planar barriers which could serve to inhibit the propagation of an electrical tree, or some related damage structure. However, it is not so easy to explain why a low concentration of spherulites should result in reduced electrical strength.

It is well appreciated that contaminant particles will inevitably become incorporated into high voltage insulation during commercial manufacturing processes and, therefore, many studies have been performed to examine the influence of inclusions on dielectric breakdown [36–38]. In 1988 Morshuis *et al.* [38] reported on a comparative study of the effects of a range of metallic, biological and mineral particles and concluded that glass was most deleterious in high voltage applications. In the absence of any firm evidence, this surprising result (the stress enhancement in the vicinity of a metallic inclusion should be far more severe than that arising from the permittivity mismatch between a polymer and a fragment of an inorganic glass) was attributed to void formation as a consequence of debonding at the interface between the matrix and the inclusion. In the case of linear polyethylene spherulites within a branched polyethylene matrix, this seems implausible. However, other arguments, based upon differential coefficients of expansion, the specific volume changes associated with crystallization, permittivity mismatches, etc. also seem inappropriate in the systems considered here. In view of this, we propose a morphological explanation for the reduction in electrical strength we see when small LPE-rich inclusions are allowed to develop.

Consider for example BPA 124/20, as shown in Fig. 8b. Clearly, the structure of the matrix that developed on quenching, differs from that of the analogous quenched specimen (BPA Q/20; Fig. 9), since there is no evidence of large scale spherulitic structures within the BPE-rich phase of the isothermally crystallized specimen. We therefore propose that this morphological change (which is likely to be related to nucleation processes) results in a reduction in the local electrical strength of the BPE-rich phase of BPA 124/20, relative to that of BPA Q/20. Below 17%, at a crystallization temperature of 124 °C, the reduction in strength of this matrix material more than offsets the reinforcing effect of the LPE-rich inclusions, such that the material as a whole becomes electrically weaker. Above 17%, it is the strength of the linear polyethylene inclusions that dominate. A similar argument can be applied to the 115 °C specimens, but here, the spherulites tend to dominate at only 7% LPE. Thus, by considering these specimens in terms of a two-phase model (reinforcing LPE-rich inclusions within a weakened BPE-rich matrix) it is possible to account for the observed behaviour. Overall, these trends lead to the important conclusion: *morphological changes result in changes in electrical strength.*

Having discussed the variation in electrical strength seen in the isothermally crystallized materials, some comment is necessary concerning the invariance seen in the quenched samples. This result directly supports the argument presented above. As far as the measured electrical strength is concerned, even appreciable changes (i.e. the addition of 20% linear polymer) in the molecular composition of the blend are unimportant, *provided they do not result in a change in morphology.*

Although the mechanisms by which morphology influences dielectric strength are poorly understood, it is nevertheless clear that blending has considerable potential as a scientific expedient for exploring structure/electrical property relationships, and as a technological means of preparing enhanced polyethylene insulation materials. In this work, breakdown strength has been used as a measure of performance, but the results concur with those reported by Nitta and Funayama [39] who measured inception voltages in a number of polyethylene blends. Although no details of materials or processing routes were provided in their paper, a similar general improvement in the performance of the blends with increasing linear polyethylene content was reported.

4. Conclusions

We have shown how blending can be used to produce two phase morphologies with, to a first approximation,

constant composition spherulites and matrix. Isothermal crystallization results in linear rich inclusions distributed in a branched polyethylene matrix; the number and size of the LPE-rich domains are found to increase with linear content and, ultimately, isothermal crystallization is simply limited by the amount of LPE present in the system. No clear structural variations were observed in the case of quenched samples; all specimens exhibited a similar banded spherulitic morphology. By exploiting this ability to design the lamellar textures within a particular sample, it has been possible for the first time to deconvolve the role of the spherulitic morphology in influencing dielectric breakdown from that of any defective, impurity rich, interspherulitic regions. In this study, the small variations in the matrix composition that do occur are unlikely to be important *per se*, since quenching shows that the molecular composition has little bearing on electrical strength, provided the morphology remains unchanged.

Although performance generally improves with increased linear content, detrimental effects were seen in low linear content blends, where only a few small spherulitic structures were present. This general form of behaviour was similar for both isothermally crystallized blend systems and could be attributed to structural changes within the interspherulitic matrix. Space-filling open banded spherulites gave the greatest increase (noted above 7%) in electrical strength, whereas compact spherulites which did not interpenetrate were less beneficial. These results are consistent with a failure route involving the growth of an electrical tree, or some related structure; the spherulites either cause the tree to adopt a more extended, meandering path or, in the extreme cases where they impinge, force the tree to penetrate the highly crystalline material.

In summary, the number, size and type of spherulites introduced have profound consequences for the electrical strength of the blend. Variations in molecular composition on their own, have little effect. If the linear content is chosen to be high, and the sample is crystallized to increase the size and number of the spherulites that are present, a significant improvement in electrical strength can be obtained over the branched material alone. This could have wide ranging implications for cable manufacturers, if a commercially viable production route can be devised. This, and other issues associated with morphology, molecular composition and electrical strength will be addressed in subsequent publications.

Acknowledgements

The authors wish to thank The National Grid Company plc (NGC) for giving permission to publish the results. One of us (I.L.H.) would like to thank the Science and Engineering Research Council and NGC for the receipt of a CASE studentship.

References

1. D. R. PAUL and S. NEWMAN, "Polymer Blends" Vol. 1 (Academic Press, New York, 1978).
2. *Idem*., "Polymer Blends" Vol. 2 (Academic Press, New York, 1978).
3. D. J. WALSH "Comprehensive polymer science. Volume 2 – Polymer Properties", edited by C. Booth and C. Price (Pergamon Press, Oxford, 1989), p. 135.
4. M. J. HILL, P. J. BARHAM, A. KELLER, and C. C. A. ROSNEY, *Polymer* **32** (1991) 1394.
5. J. M. REGO-LOPEZ, M. T. CONDE-BRANA, B. TERSELIUS and U. W. GEDDE, *ibid*. **28** (1988) 1045.
6. D. R. NORTON and A. KELLER, *J. Mater. Sci.* **19** (1984) 447.
7. A. S. VAUGHAN, *Polymer* **33** (1992) 2513.
8. G. KRAUSE, D. MEURER and D. KLEE, *IEEE. Trans. Electr. Insul.* **24** (1989) 419.
9. M. NAGAO, I. KONBA, T. TSURIMOTO, Y. MIZUNO and M. KOSAKI in Annual Report of Conference on Electrical Insulation and Dielectric Phenomena, Victoria BC, Canada 1992, p. 148.
10. E. A. FRANKE, J. R. STAUFFER and E. CZEKAJ, *IEEE Trans. Electr. Insul.* **12** (1977) 218.
11. P. J. PHILLIPS, *ibid*. **13** (1978) 69.
12. P. FISCHER, in "Electrical Properties of Polymers", edited by D. A. Seanor (Academic Press, New York, 1982) p. 319.
13. C. C. KU and R. LIEPINS " Electrical Properties of Polymers" (Hanser, Munich, 1987).
14. R. COOPER, B. R. VARLOW, D. R. EDWARDS, P. B. MACALLISTER and T. J. CARTER, in Annual Report of Conference on Electrical Insulation and Dielectric Phenomena, Boston MA (1980) p. 220.
15. P. H. H. FISCHER and K. W. NISSEN, *IEEE Trans. Electr. Insul.* **11** (1976) 37.
16. S. N. KOLESOV, *ibid*. **15** (1980) 382.
17. H. WAGNER in 1974 Annual Report of Conference on Electrical Insulation and Dielectric Phenomena (IEEE, Washington DC, 1975) p. 62.
18. B. V. CERES and J. M. SCHULTZ, *J. Appl. Polym. Sci.* **29** (1984) 4183.
19. J. H. MASON, *IEEE Trans. Electr. Insul*. **26** (1991) 318.
20. D. FOURNIER and L. LAMARRE in Proceedings DMMA, IEE Conference Publication 363, (IEE, London, 1992), p. 330.
21. R. H. OLLEY and D. C. BASSETT *Proc. R. Soc. Lond. A* **359** (1978) 121.
22. J. H. M. WILLISON and A. J. ROWE, in "Practical methods in electron microscopy, Volume 8: Shadowing and Freeze Etching Techniques", edited by A.M. Glauent (North Holland, Amsterdam, 1980).
23. R. D. NAYBOUR, *IEEE Trans. Electr. Insul.* **13** (1978) 59.
24. L. A. DISSADO and J. C. FOTHERGILL, in "Electrical degradation and breakdown in polymers", edited by G.C. Stevens (Peter Peregrinus, London, 1992).
25. A. GUSTAFSSON and U. W. GEDDE, in Proceedings of the Nordic Insulation Symposium (Vasteras, 1992) p. 8.4: 1.
26. W. L. WADE, R. J. MAMMONE and M. BINDER, *Polymer* **34** (1993) 1093.
27. S. R. HU, T. KYU and R. S. STEIN, *J. Polym. Sci.*: *Part B*; *Polym. Phys.* **25** (1987) 71.
28. J. D. HOFFMAN, G. T. DAVIS and J. I. LAURITZEN, "Treatise on solid state chemistry, Volume 3: Crystalline and Non-crystalline Solids", edited by N. B. Hannay (Plenum, New York, 1976) p. 497.
29. H. D. KEITH and F. J. PADDEN, *J. Appl. Phys.* **35** (1964) 1270.
30. J. R. DRYDEN, *J. Mater. Sci. Lett*. **6** (1987) 1129.
31. D. PATEL and D. C. BASSETT, *Proc. R. Soc. Lond. A* **445** (1994) 577.
32. P. J. BARHAM, M. J. HILL, and C. C. A. ROSNEY, *J. Mater. Sci. Lett*. **7** (1988) 1271.
33. W. GOLZ, *Colloid and Polym. Sci.* **263** (1985) 286.
34. N. HOZUMI, T. OKAMOTO and H. FUKAGAWA, *Jpn. J. Appl. Phys.* **27** (1988) 1230.

35. N. HOZUMI, M. ISHIDA, T. OKAMOTO and M. FUKAGAWA, *IEEE Trans. Electr. Insul.* **25** (1990) 707.
36. C. LAURENT and E. KAY, *J. Appl. Phys.* **64** (1988) 336.
37. T. NENSI, A. E. DAVIES, A. S. VAUGHAN and S. G. SWINGLER in Annual Report of Conference on Electrical Insulation and Dielectric Phenomena (IEEE, Victoria, BC, Canada, 1992) p. 493.
38. P. H. F. MORSHIUS, F. H. KREUGER and P. P. LEUFKINS, *IEEE. Trans. Elect. Insul.* **23** (1988) 1051.
39. Y. NITTA and M. FUNEYAMA, *ibid.* **13** (1978) 130.

Received 21 October 1996
and accepted 18 February 1997